UDC 533.6.013.14 : 629.1.025.3 https://doi.org/10.15407/itm2023.01.040

G. O. STRELNIKOV, N. S. PRYADKO, K. V. TERNOVA

Institute of Technical Mechanics
of the National Academy of Sciences of Ukraine and the State Space Agency of Ukraine,
st. Leshko-Popelya, 15, 49005, Dnipro, Ukraine; e-mail: np-2006@ukr.net

WAVE STRUCTURE OF THE GAS FLOW IN A TRUNCATED NOZZLE WITH A LONG BELL-SHAPED TIP

В останні роки все більше уваги привертають сопла з нетрадиційним контуром, що відрізняються від контуру класичного сопла Лаваля, спрофільованого за лініями струму. У таких соплах поля течії, як правило, включають надзвукові і дозвукові потоки, що взаємодіють, найчастіше з рециркуляційними областями і складною хвильовою структурою потоку.

У цій роботі чисельно досліджується хвильова структура течії газу в надзвуковому укороченому соплі з дзвоноподібним насадком еліптичної форми та великої довжини (порівняно з конічною ділянкою на вході в насадок). Моделюється потік газу всередині сопла та у зовнішньому просторі з використанням пакету прикладних програм «ANSYS». Розрахунки проведені в нестаціонарній вісьосиметричній постановці на основі усереднених за Рейнольдсом рівнянь Навье–Стокса, замкнених з використанням SST-моделі турбулентності з функціями пристінок і поправкою на стисливість. У розрахунках варіювались тиски на вході в сопло та зовнішнього середовища. Коректність методичних підходів до вирішення завдання досліджень верифікована у попередніх роботах авторів.

Результати досліджень показали таке. При невеликих значеннях тиску на вході в сопло (P_0<50 бар) та зовнішньому тиску 1 бар на стінці насадка існує розвинена відривна зона з великомасштабним і дрібномасштабним (в області зрізу насадка) вихорами. В області першої «бочки» потоку газу із сопла існує «сідлоподібна» хвильова структура стиснення малої інтенсивності. При відривній течії тиск на стінці в зоні відриву на ~ 15 % менше тиску зовнішнього середовища. При P_0>100 бар тиск у потоці на стінці насадка змінюється практично пропорційно тиску на вході в сопло. При роботі у верхніх шарах атмосфери статичний тиск газу у поперечному перерізі на зрізі насадка монотонно зменшується, починаючи від осі сопла до точки мінімуму значення тиску, потім лінійно зростає до максимального значення на стінці насадка. При відривній течії в насадку при роботі на рівні моря статичний тиск газу у вказаному перерізі має такий же характер для вхідного тиску P_0>50 бар. При P_0=50 бар існує дві точки зміни характеру статичного тиску: від осі тиск монотонно зменшується до мінімуму значення у першій точці, яка знаходиться ближче до осі потоку, далі тиск збільшується до другої додаткової точки, в якій тиск досягає максимального значення і далі незначно зменшується до стінки насадку.

.

Ключові слова*: укорочене надзвукове сопло, дзвоноподібний насадок, розподіл статичного тиску, ударна хвиля, тиск зовнішнього середовища.*

In recent years, more and more attention has been paid to nozzles with an unconventional profile, which differs from that of the classical streamline-profiled Laval nozzle. In such nozzles, the flow fields typically include interacting supersonic and subsonic flows, often with recirculation regions and a complex wave structure of the flow.

This work is concerned with a numerical study of the wave structure of the gas flow in a truncated supersonic nozzle with an elliptical bell-shaped tip whose length is long in comparison with the conical section upstream of the tip. The gas flow inside the nozzle and in the surrounding space was simulated using the ANSYS software package. The calculations were carried out in a non-stationary axisymmetric formulation based on the Reynolds-averaged Navier–Stokes equations closed with the use of the SST turbulence model with near-wall functions and a compressibility correction. In the calculations, the nozzle inlet pressure and the ambient pressure were varied. The correctness of the methodological approaches to the solution of the problem was confirmed in the authors' previous works.

The study showed the following. At low values of the nozzle inlet pressure (P_0 < 50 bar) and an ambient pressure of 1 bar, the tip wall exhibits a developed separation zone with a large-scale vortex and a small-scale one (near the tip exit). The first "barrel" of the outflowing gas shows a "saddle" low-intensity compression wave structure. In the case of a separated flow, the tip wall pressure in the separation zone is about 15% less than the ambient pressure. At P_0 > 100 bar, the tip wall pressure is nearly proportional to the nozzle inlet pressure. In the upper atmosphere, when going in a radial direction from the nozzle axis at the tip exit cross-section, the static pressure monotonically decreases, reaches a minimum, and then increases linearly to the its maximum value on the tip wall. In the case of a separated flow in the tip at a sea-level ambient pressure, the static pressure at the tip exit cross-section behaves in the same manner for inlet pressures P_0 > 50 bar. At P_0 = 50 bar, there exist two extrema: the pressure first deceases to its minimum value, then increases to its maximum value, and then decreases slightly to its value on the tip wall.

Keywords: *truncated supersonic nozzle, bell-shaped tip, static pressure distribution, nozzle thrust characteristic, ambient pressure.*

Introduction. The choice and justification of the nozzle design is one of the important tasks in the design and optimization of rocket characteristics. The complexity of flows in different types of nozzles remains a major problem. In shortened nozzles, the flow fields, as a rule, include interacting supersonic and subsonic flows, often with recirculation regions and a complex wave structure of the flow. The creation of various nozzle configurations has several goals: improving the energy characteristics of the propulsion system, in particular, the specific thrust impulse; optimization of performance under various operating conditions – in the sea level conditions and in conditions of high altitude; improvement of the nozzle design in conditions of a dense engine layout to increase the rocket payload. In accordance with these goals, various nozzle shapes are being developed.

In practice, various technical solutions are used to increase the expansion ratio of the nozzle. Under the conditions of dimensional restrictions imposed on the longitudinal and transverse dimensions of the rocket, the coefficient of geometric tip expansion is increased by using design schemes of tips with a variable expansion degree, with rigid retractable nozzles, flexible nozzles, and petal rosettes [1].

Recently, duel bell nozzles have been considered very promising for improving rocket nozzle performance compared to conventional nozzles [2]. Double flare nozzles allow two different modes of operation that provide higher performance than conventional flare nozzles for sea level rocket engines [3]. In low-altitude mode, flow separation occurs, and the separation line is located near the nozzle wall inflection, in the area characterized by a negative pressure gradient on the wall, as in conventional nozzles, and in which side loads are possible [4].

Previous [5] studies of the gas flow characteristics in a shortened nozzle with a bell-shaped nozzle showed a significant difference in the characteristics of the flow in it from the Laval nozzle of the traditional configuration, profiled along the streamline. In such a nozzle, separation of the flow from the wall is possible with the formation of rarefaction waves and shock waves of various nature. The agreement between the calculations of the characteristics of shortened nozzles and the experiment was also confirmed in previous studies by the authors [5]. The model of flow turbulence optimal for calculations of such flows was also chosen there, and studies of the influence of gas properties on the calculated characteristics of the flow structure in unconventional nozzle configurations were carried out.

In recent years, nozzles with an unconventional contour, the so-called “dual bell nozzle” nozzles (double expansion bell-shaped nozzle) [6], have attracted increasing attention. The studies of these nozzles are carried out using modern numerical simulation software and modern experiment. Such nozzles have been studied earlier [7]. In this case, it was necessary to consider the features inherent in such nozzles, in particular, separated flows in them

An increase in the geometric expansion ratio of the nozzle leads to an over expanded flow regime inside the nozzle, when the static pressure in a significant part of the circuit is less than the pressure in the outside of nozzle (in this part of the circuit, a negative contribution to the nozzle thrust is realized), separation of the flow from the wall with the formation of shock waves and secondary flows [8]. For nozzle blocks with a large degree of geometric expansion, it becomes possible for the occurrence of dynamic high-frequency side loads with pressure increase in the combustion chamber at the start-up stage.

However, it is also possible to achieve an increase in the geometric expansion degree with other modifications of standard nozzles, in particular, using various

tips for shortened nozzles [5]. Nozzles of these configurations, which tips follow the shape of the combustion chamber, can be used in rocket engines with a dense layout, which allows reducing the mass of the engine.

For the calculation of nozzles, the method of characteristics has been widely used for a long time [9]. However, unexpected flow expansion in subsonic and supersonic conditions is a major problem in aerospace applications. Computational fluid dynamics (CFD) is a promising method for modeling and simulating flow fields, which makes it possible to obtain reliable results regarding the flow characteristics of nozzles of various designs [10].

The purpose of the work is to determine the wave structure of the gas (air) flow in the supersonic region of a shortened nozzle with a bell-shaped tip.

The paper studies the features of a supersonic flow at various initial pressures P_0 and various external medium conditions - at sea level (pressure of the external medium behind the nozzle exit $P_н$ = 1 bar) and high-altitude layers of the atmosphere ($P_н$ = 0.1 bar and $P_н$ = 0.01 bar). The gas flow inside the nozzle is simulated with the subsequent outflow of the jet into the surrounding space using the ANSYS software package.

Geometric model and computational technique. The geometric model is based on the experimental nozzle given in [5], where the calculations of the flow characteristics in the nozzle were verified with experimental data.

The nozzle in the expanding supersonic part is made in the form of a cone with a half-angle of 20^0. In contrast to [5], the length of the conical part along the axis was taken 5 mm. In this work, the same bell-shaped tip is used. The radius of the exit section of the tip is 28 mm. The size of the critical section of the nozzle is 10 mm. The coefficient of geometric expansion is 5.6. The total length of the supersonic part of the nozzle is 35 mm. The nozzle contour is approximated by a polynomial (with the origin at the corner point in the critical section of the nozzle) y=-0.03x^2+1.8453x-0.8466 with a correlation coefficient of 0.9966. The tip wall angle at the cut relative to the nozzle axis is 0^0, the tip cut diameter is 56 mm. The half-opening angle of the input conical part is 20^0.

The calculations are carried out on a section of 30L × 15L, where L is the length of the nozzle. In [5], a sufficient accuracy of the gas flow calculations in such a nozzle in an axisymmetric formulation was shown.

The computational area consists of two blocks, one of which is used to simulate the flow in the nozzle, and the other allows taking into account the outflow of the jet into the surrounding space. The use of an extended computational area makes it possible to reproduce the flow structure not only in the nozzle, but also behind its outlet affected the characteristics of the flow in the nozzle [5].

The calculations were carried out in a non-stationary axisymmetric formulation based on the Reynolds averaged Navier–Stokes equations closed by using the SST turbulence model with near-wall functions and correction for compressibility. The choice of the mentioned turbulence model is due to the analysis carried out in [11] and the choice of the most optimal model for the flow in similar nozzles under study. Air is used as the working medium.

To control the convergence of the iterative process, the level of discrepancy of the searched functions is checked. Calculations stop when the residual level of all necessary functions reaches 0.0001. The total number of iterations depends on the environmental conditions (P_n) and ranges from 100 to 800 iterations.

Main part. Fig. 1, a), b), c) shows the distributions of Mach numbers M, velocity V, and flow density ρ at a nozzle inlet pressure P_0 = 50 bar and external pressure $P_н$ = 1 bar. An analysis of the distribution of M and V shows the following. In the inlet conical part of the nozzle, a preliminary expansion of the gas flow occurs with a sound line convex towards the nozzle outlet. Behind the end of the conical inlet section of the nozzle, there is a pattern of outflow of a flow underexpanded in the nozzle with a wave structure characteristic of this case

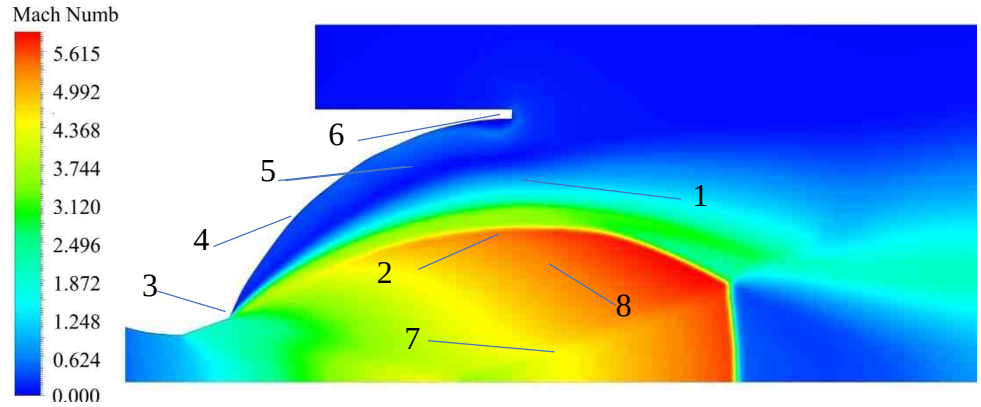

a)

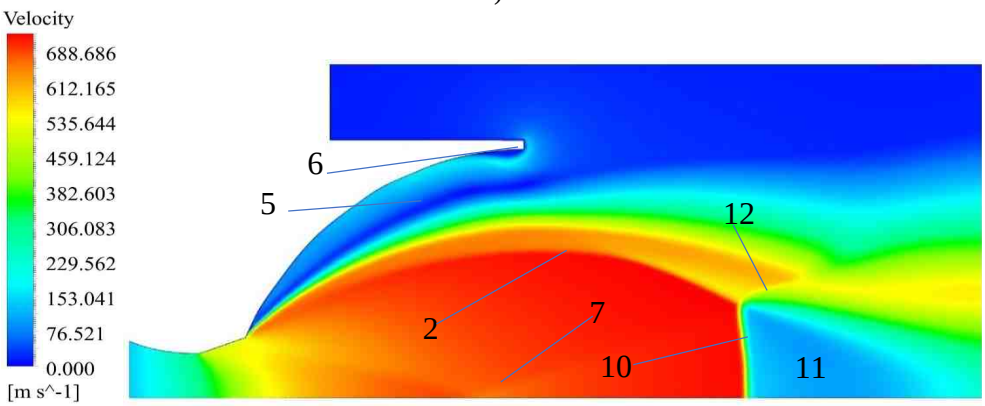

b)

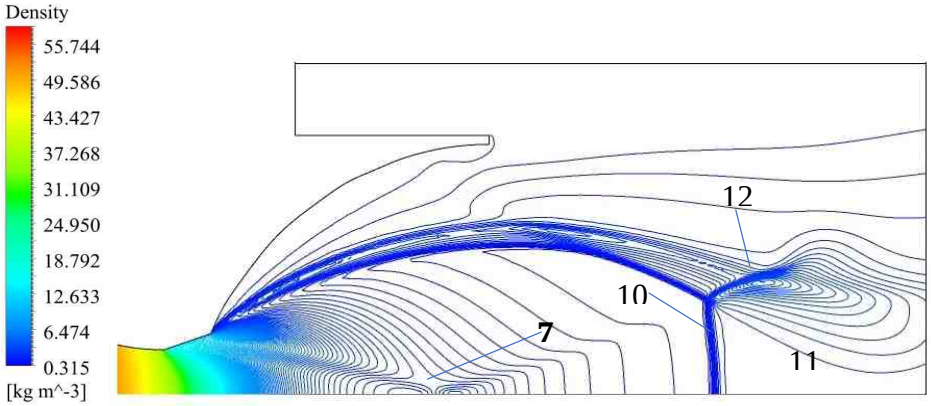

c)

Fig. 1 – Distribution of Mach numbers (a), velocity (b) and density (c) in a gas flow at P_0 = 50 bar and external pressure $P_н$ =1 bar

In front of the free boundary 1 of the jet flowing out of the nozzle, a hanging shock 2 is observed, caused by a beam of converging characteristics. The jump is a consequence of the characteristic reflection that appear near the exit edge of the nozzle from the free boundary of the jet [12]. Behind the corner point 3 of the entrance to the tip 4 there is a zone 5 of developed flow separation from the wall of the tip. At the tip end, a small zone of secondary vortex 6 is formed, which is caused by a large gradient of change in the tip contour angle. In the core of the gas jet, the flow accelerates unevenly, high speeds up to M = 5.5 are observed in the peripheral zone 8 of the jet. On the flow axis in the direction of the tip cut in zone 7, the flow velocity is lower compared to zone 8. This is explained by the existence of a low-intensity hanging “saddle-shaped” shock in the core of the gas flow behind the end of the inlet conical part of the nozzle. Hanging shock 2 (Fig. 1, a), b)) is caused by supersonic compression from a beam of converging characteristics reflected from the free boundary of the jet. The hanging shock 2 is closed by the Mach disk 10, behind which the flow becomes subsonic in zone 11. Behind the reflected shock 12, as well as behind the disk 10, the flow velocity is subsonic, and the pressure is higher than the surrounding $P_н$. Therefore, behind them (disk and shock), the gas flow accelerates again, forming a second "barrel" of less intensity. This is explained by the wave energy losses of the flow in the first "barrel".

The distribution of velocity vectors in the flow (Fig. 2 a) clearly demonstrates the vortex structure in the zone of flow separation from the tip wall.

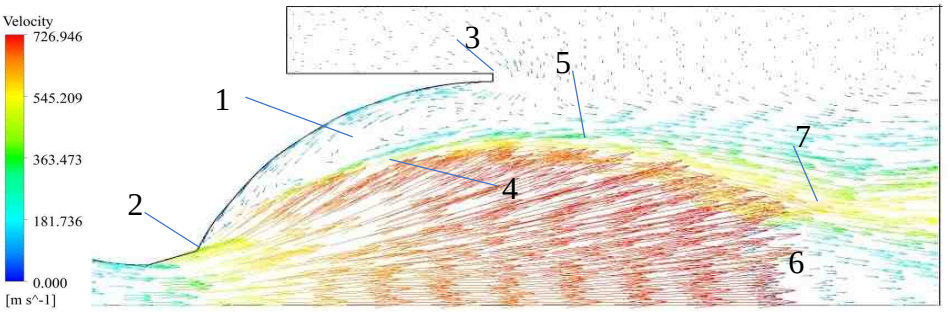

a)

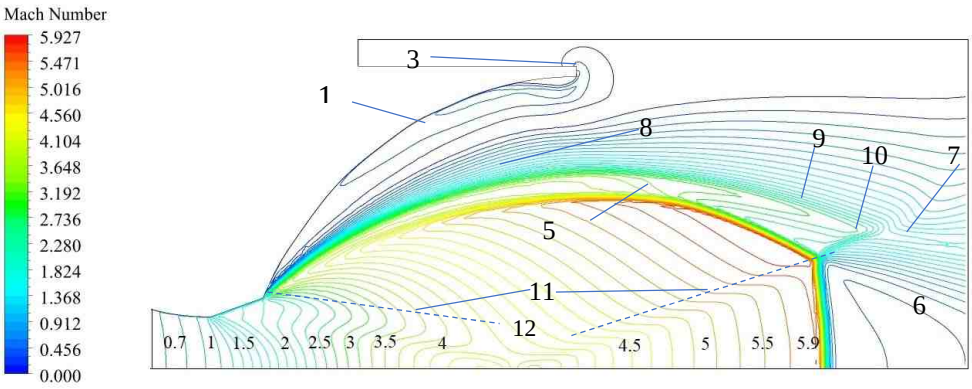

b)

Fig. 2 – Distribution of velocity vectors (a) and isolines of Mach numbers (b) in the flow at P_0=50 bar, $P_н$=1 bar

Here, there are two vortices: large-scale 1 originating from the corner point 2 of the tip inlet, and small-scale vortex 3 (or 6 in Fig. 1, a)) at the exit edge of the tip. In a “saddle” hanging shock (12 in Fig. 2, b)) and 7 in Fig. 1, b)), the velocity

vectors practically do not deviate along the streamline. The deviation of the vectors in the streamlines is observed on the hanging shock 4, in the vortex zone 5, and on the free boundary 5 of the gas flow (Fig. 2, a), b)). At the periphery of the subsonic zone 6, the flow accelerates again in zone 7, which corresponds to the Mach number (M = 5.3) of the isentropically expanded gas flow.

Figure 2, b) shows a picture of the isolines of the Mach number in the flow. The "saddle-shaped" hanging shock mentioned above is characterized by anomalous behavior of isolines. The envelope 11 of the isoline maxima in the region of the "saddle" shock forms zone 12 with a constant velocity on the nozzle axis in the region close to the nozzle exit. This "saddle-shaped" hanging shock is clearly visible in Fig. 2, a) with the velocity distributions in the flow. In these figures, hanging shocks are also clearly visible, limiting the first "barrel" in the jet flowing from the nozzle. After the first barrel there follow the periodic acceleration and deceleration of the flow, which decays downstream, where the flow pressure equalizes with the ambient pressure

Figure 2 b) also refines the flow structure in separation zone 1 (zone 5 in Fig. 1, a), b)). The external flow enters the tip with the maximum speed in the middle part of the separation zone (between the free boundary of the supersonic jet flowing from the shortened conical part of the nozzle and the tip wall). Thus, a large-scale vortex 1 is formed (Fig. 2, a), b)) between the free boundary of the jet and the tip wall. A small-scale separation zone 3 is formed near the tip end on its wall (Fig. 2, a); zone 6 in Fig. 1, a)).

From Fig. 2 b) it follows that the flow within the wave structure of the first barrel expands (according to the isolines) up to M = 5.9, i.e. more than with isentropic expansion to the tip area (M = 5.3). This discrepancy can be explained by the additional nonisentropic expansion of the flow in zone 9 (Fig. 2, a)) up to the secondary hanging shock 8, which has moved away from the tip wall. Reflected shock 10 is formed at the end of zone 9. Estimates of the flow expansion degree according to one-dimensional theory show that an increase in the transverse area bounded by hanging shocks 1 and 8 corresponds to an increase in the Mach number within the first barrel from M = 5.3 to M = 5.9. Indeed: the Mach number M = 5.3 corresponds to $q_1 = \left(\frac{d_*}{D_a}\right)^2 \approx \left(\frac{d_*}{d_1}\right)^2 = 3.19 \cdot 10^{-2}$. The Mach number M = 5.9 corresponds to $q_2 = \left(\frac{d_*}{d_2}\right)^2 = 2.04 \cdot 10^{-2}$, where (on the scale of Fig. 2, b)) d_1 = 15.9 mm is the diameter of the hanging shock 1 the first barrel in its maximum section; d_2 = 19.5 mm is the diameter of the secondary shock 8 in the same section of the gas flow.

Figure 3 shows the distribution of Mach numbers in the gas flow at P_0 = 50 bar, $P_н$ = 0.1 bar.

On the tip wall the flow is unseparated, the hanging shock 1 originates from the corner point 2 of entry into the tip and extends to the cut 3 of the tip, almost equidistant to the tip wall. Behind the shock 1 in front of the nozzle wall, a zone 4 of low velocity and high pressure is formed, caused by the turn of the flow in the shock. Behind the tip end, the flow from zone 4 with increased pressure flows out of the nozzle with the formation of an expanding stream 5. This flow distorts the shape of the hanging shock 1, in other words, it deforms the first “barrel” of the

supersonic flow just after the tip end 6. The free boundary 7 of the flow behind the cut deviates from the axis by an angle determined by the Prandtl–Meyer flow at the corner point of the tip cut. The decrease in the intensity of the hanging shock 1 with approaching the corner point 2 (upstream) of the tip inlet is explained by the decrease in the radial displacement of the flow streamlines, which leads to a weakening of the flow overexpansion just behind the corner point 2. The longitudinal dimensions of the first (distorted) "barrel" significantly exceed the dimensions of the barrel at $P_н$ = 1.0 bar.

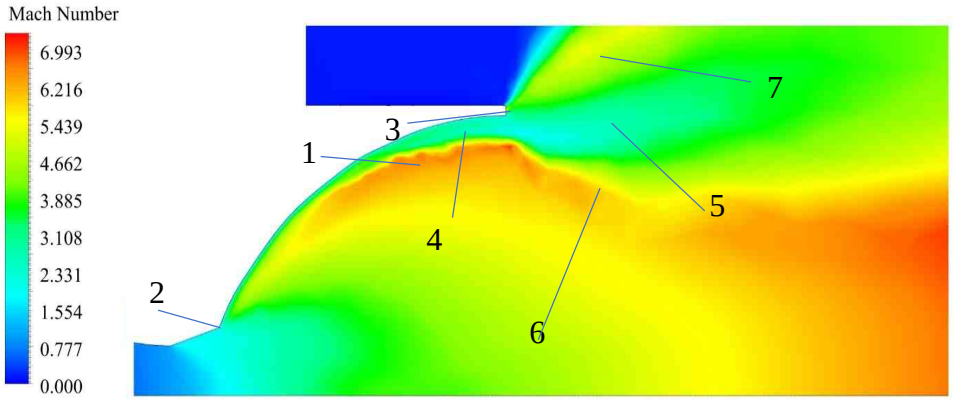

Fig. 3 – Distribution of Mach numbers in gas flow at P_0 = 50 bar, $P_н$ = 0.1 bar

Figure 4 shows the distribution of Mach numbers in the flow at P_0 = 50 bar, $P_н$ = 0.01 bar. With a decrease in external pressure from $P_н$ = 0.1 to $P_н$ = 0.01 bar, the configuration of the first "barrel" in the flow practically does not change. The flow at the free boundary changes in proportion to the decrease in external pressure. The free boundary 1 deviates in the Prandtl-Meier current by a correspondingly larger angle. The flow rate in zone 2 also increases in proportion to $P_н$. In this case, it should be noted that there is practically no “saddle-shaped” wave structure in the first “barrel” of the flow at $P_н$ = 0.1 bar and $P_н$ = 0.01 bar. This is due to a more uniform radial expansion of the flow within the first "barrel".

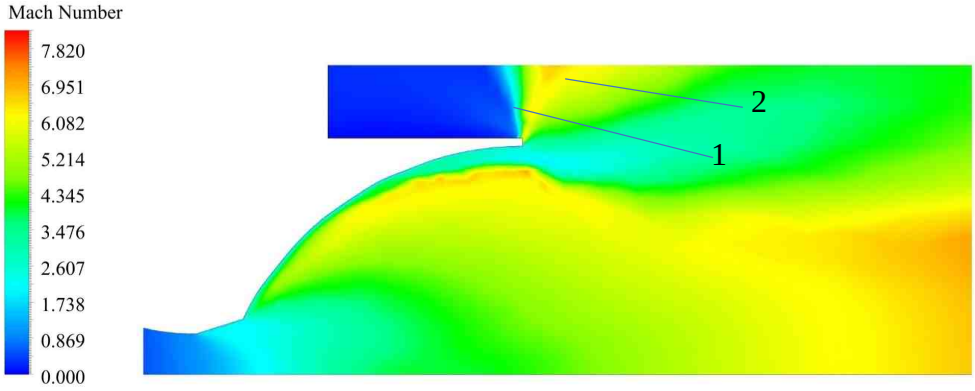

Fig. 4 – Distribution of Mach numbers in the gas flow at P_0 = 50 bar, $P_н$ = 0.01 bar

Fig. 5, a) shows the distribution of Mach numbers in the flow at P_0 = 100 bar, $P_н$=1 bar. In contrast to the distribution at P_0 = 50 bar, $P_н$ = 0.1 (Fig. 3), in this case, there is no separation vortex zone (5 in Fig. 1, a)) near the tip wall, caused by the entry of the air into the tip near its wall. Zone 1 is observed near the tip wall

from the corner point of entry into it to the tip end behind a hanging (disconnected) shock 2, which is formed in front of the tip wall due to the inflow of the expanded supersonic flow onto the wall.

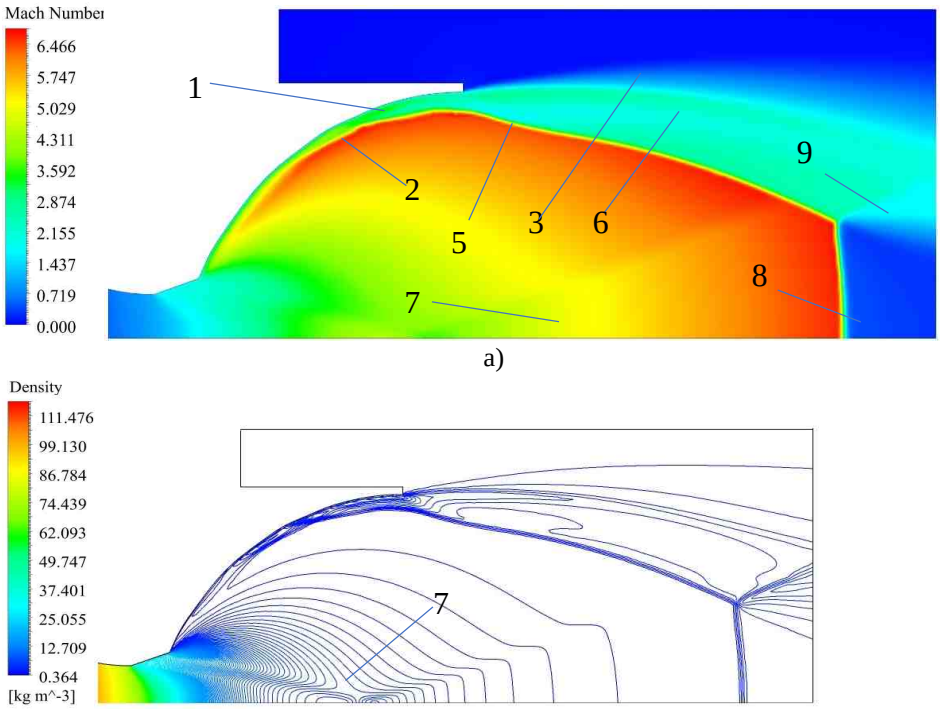

Fig. 5 – Distribution of Mach numbers (a), density (b) in a gas flow at P_0 = 100 bar and external pressure $P_н$ =1 bar

The free boundary 3 of the flow starts from the nozzle end, in contrast to the case P_0 = 50 bar, $P_н$ = 1 bar, where the free boundary starts from the corner point in the nozzles. In this case, the wave structures inside the first “barrel” (Fig. 5, a) and Fig. 1, a)) are similar. A similar jet structure is also observed in the far track behind the first “barrel”. The length of the first “barrel” compared to P_0 = 50 bar (Fig. 1, a)) increases in proportion to the increase in inlet pressure, i.e. doubled (Fig. 5, a)) and is closed by a Mach disk 8. At the base of the Mach disk, a reflected shock 9 is observed. This is explained by the action of a high-pressure flow from zone 1 of flow stagnation near the nozzle wall behind the detached shock wave 2 (Fig. 5, a). This also causes a change in the structure of zone 6 (Fig. 5, a)) and its transverse dimensions compared to the case P_0 = 50 bar, $P_н$ = 1 bar (Fig. 1, b)). The wave structures inside the first “barrel” are similar according to Mach number distribution in the flow at sea level at P_0 = 50 bar (Fig. 1, a)) and P_0 = 100 bar (Fig. 5, a), b)). In both cases, inside the first "barrel" there is a "saddle-shaped" compression wave 7 of similar geometry.

Figure 6, a), b) shows the velocity field and the density distribution of the flow for P_0=200 bar and $P_н$ = 1 bar.

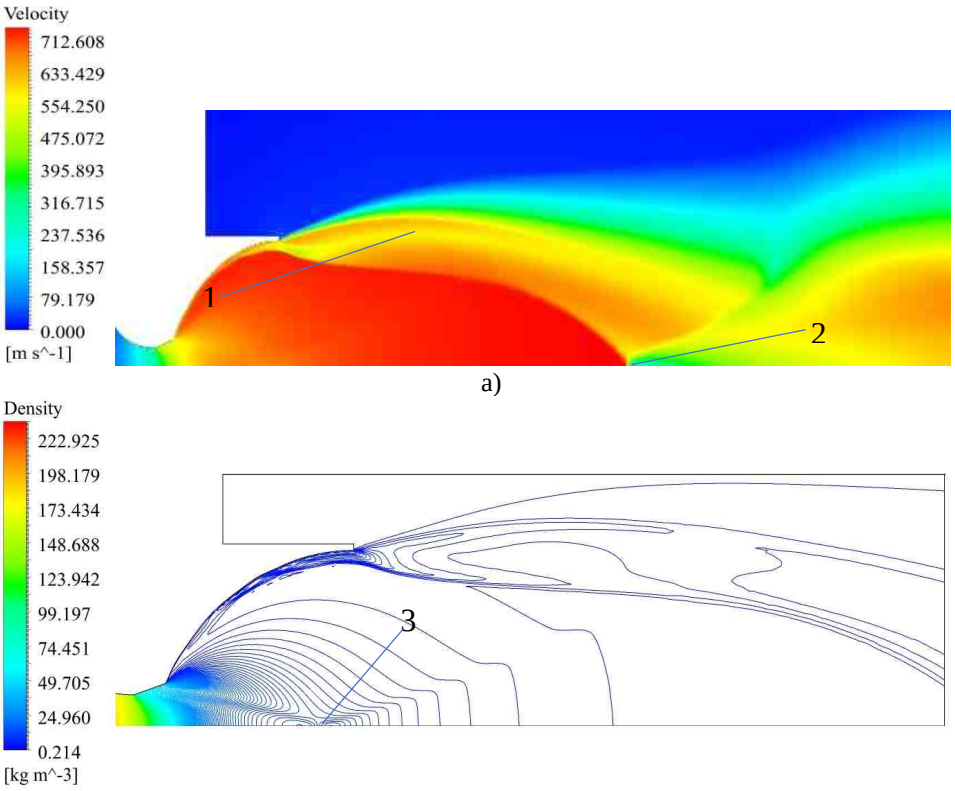

Fig. 6 – Distribution of velocity (a) and density (b) of the gas flow at P_0 = 200 bar, $P_н$ = 1.0 bar

In comparison of these parameter distribution at P_0 = 200 bar and P_0 = 100 bar (Fig. 6 and 5), a doubling of the length of the first "barrel" is observed. In this case, the transverse dimensions of zone 1 also increase in proportion to the increase in P_0. The transverse size of the Mach disk 2 (Fig. 6, a)) decreases in comparison with the case P_0 = 100 bar (Fig. 4).

Wave structure 3 inside the first “barrel” (Fig. 6, b)) remains similar to structure 7 in the case of P_0 = 50 bar (Fig. 1, b)) and P_0 = 100 bar (Fig. 5, b). In this case, the relative (to the length of the first “barrel”) longitudinal dimensions of the “saddle” wave structure 3 decrease with an increase in the inlet pressure P_0 (compare Fig. 1, c) at P_0 = 50 bar, Fig. 5, b) at P_0 = 100 bar and Fig. 6, b) at P_0 =200 bar). It should be noted the change in the velocity field behind the first “barrel” at P_0 = 200 bar (Fig. 6, b)) compared to approximately the same fields at P_0 = 50 bar (Fig. 1, c)) and P_0 = 100 bar (Fig. 5, a).

A comparison of the Mach number isoline fields at $P_0/P_н$ = 50/0.1 bar (Fig. 7, a)) and $P_0/P_н$ = 50/0.01 bar (Fig. 7, b)) shows the following. In both cases, a peripheral (conical) zone 1 with an increased gas flow rate relative to the velocity on the axis is observed behind the cutoff the conical inlet (into the tip) nozzle. This zone extends to about half the length of the tip.

Further downstream, starting from Mach $M \approx 4$, the flow expands with a weakly expressed unevenness, which forms the above "saddle-shaped" compression wave inside the first "barrel". The shock wave 2 separated from the tip wall is similar in both cases in terms of geometry and intensity.

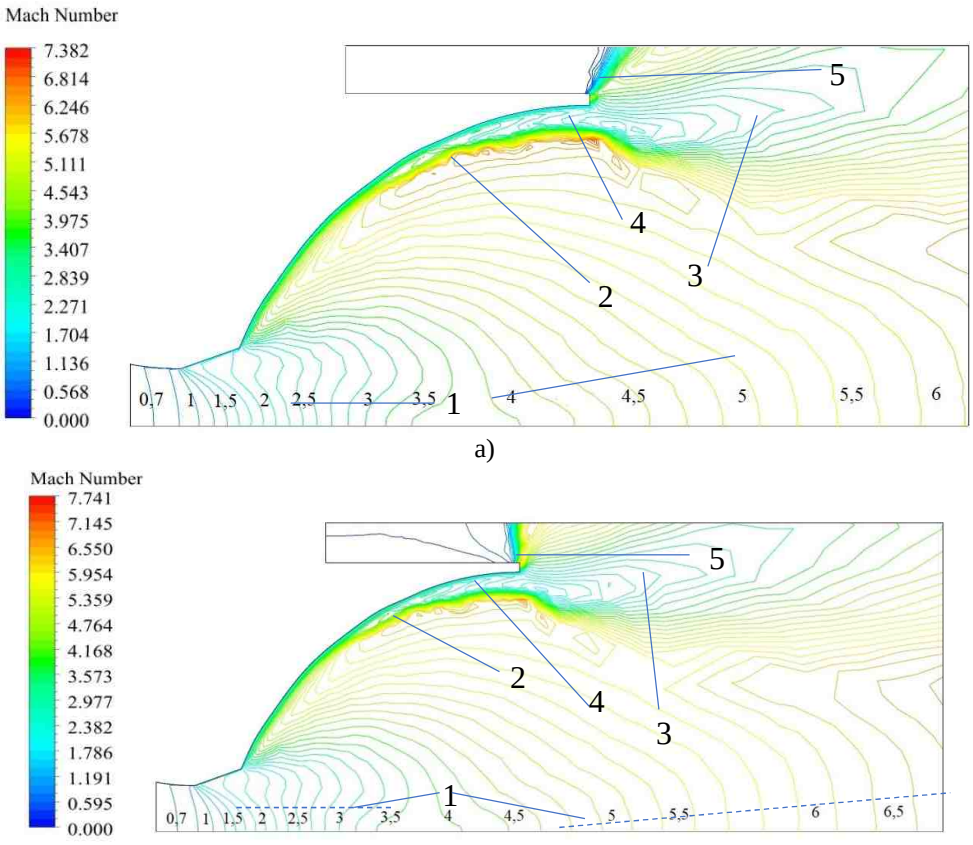

Fig. 7 – Distribution of the Mach number isoline in the gas flow at P_0 = 50 bar at $P_н$ = 0.1 bar (a) and $P_н$ = 0.01 bar (b)

Behind the nozzle cut there is a developed zone 3 of gas outflow from the zone 4 of increased pressure behind the separated (detached) shock wave 2. This outflow leads to the above-mentioned distortion of the shape of the first “barrel” behind the tip end. At the tip end edge, the gas flow expands in the Prandtl–Meyer 5 flow to the value of the turn angle corresponding to the external pressure $P_н$, i.e. larger angle for lower pressure $P_н$.

Figure 8 – 10 shows the pressure distributions on the tip wall at different scales at pressures P_0 = 50, 100, 200 bar and external pressure $P_н$ = 1 bar. The pressure on the wall of the conical nozzle section inlet to the nozzle corresponds to the pressure at the nozzle inlet P_0. The pressure on the tip wall corresponds to the described wave structure of the gas flow in the tip near its wall (Fig. 1, 5, 6). At P_0= 50 bar in the separation zone near the nozzle wall, the pressure on the wall (P_w) is almost constant and equals approximately P_w= 0.8 $P_н$ (Fig. 8). At P_0 = 100 and 200 bar, the nature of the change in pressure on the wall along the length of the tip is the same (Fig. 9, 10). The difference is only in the pressure level, which corresponds to the level P_0. When the pressure at the nozzle inlet doubles, the pressure on the tip wall also doubles.

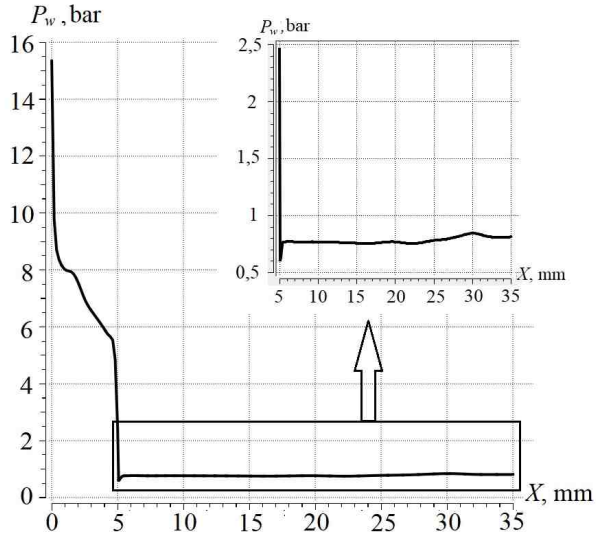

Fig. 8 – Pressure distribution on the wall of the shortened nozzle with external pressure $P_н$ = 1.0 bar and inlet pressure P_0 = 50 bar

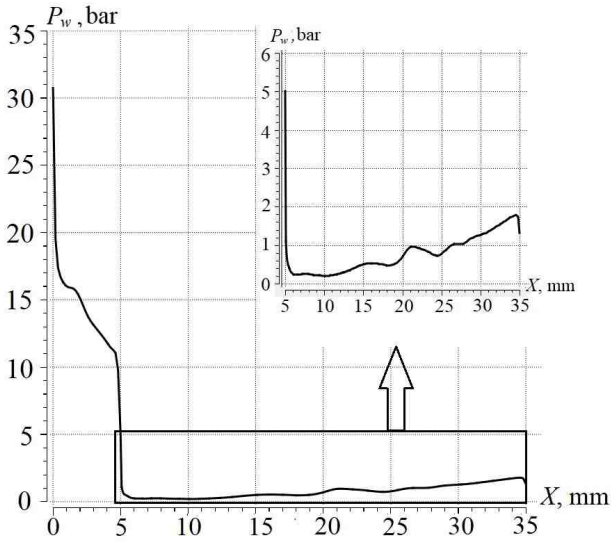

Fig. 9 – Pressure distribution on the wall of the shortened nozzle with external pressure $P_н$ = 1.0 bar and inlet pressure P_0 = 100 bar

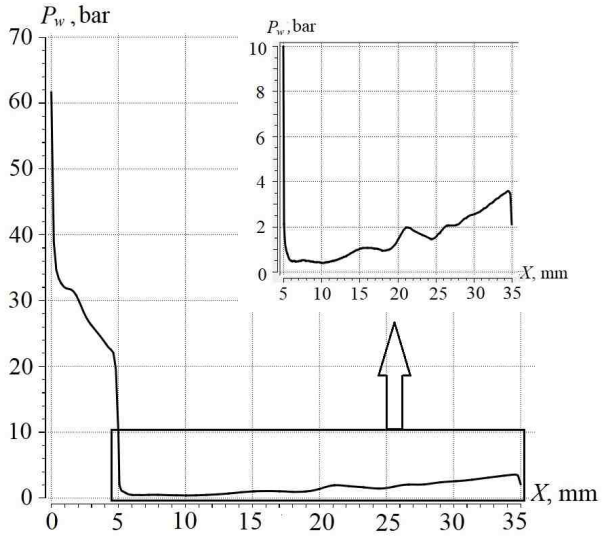

Fig. 10 – Pressure distribution on the wall of the shortened nozzle with external pressure $P_н$ = 1.0 bar and inlet pressure P_0 = 200 bar

Figure 11, a) shows the distribution of static pressure at the tip exit along the radius R at pressures in front of the nozzle P_0 = 20 bar, 50 bar, 100 bar and 200 bar and at an ambient pressure $P_н$ = 0.1 bar. As it can be seen from the graphs, their character is the same in all cases from the nozzle axis to the height ≈ 0.9R, the pressure P decreases monotonically (P is the pressure on the tip wall, R_a – radius of tip exit (end), $\overline{R} = \frac{R}{R_a}$. Up to $R = R_a$, the pressure increases linearly up to the maximum value. The pressure level P in all cases (curve 1–4) corresponds to the pressure level P_0 at the nozzle inlet.

Figure 11, b) shows the distribution of static pressure at the nozzle exit along radius R at $P_н$ = 1 and P_0 = 50 bar (curve 2), 100 bar (curve 3), 200 bar (curve 4). At P_0 = 50 bar, the pressure from the nozzle axis to $\overline{R}$ ≈ 0.57 decreases monotonically, then to $\overline{R}$ ≈ 0.8 it increases to 0.85$P_н$, after which it slightly decreases to 0.82 $P_н$ towards the tip exit. At P_0 = 100 and 200 bar, the pressure along the radius at the nozzle exit changes similarly to the change in the nozzle at $P_н$ = 0.1 bar (Fig. 11, a)).

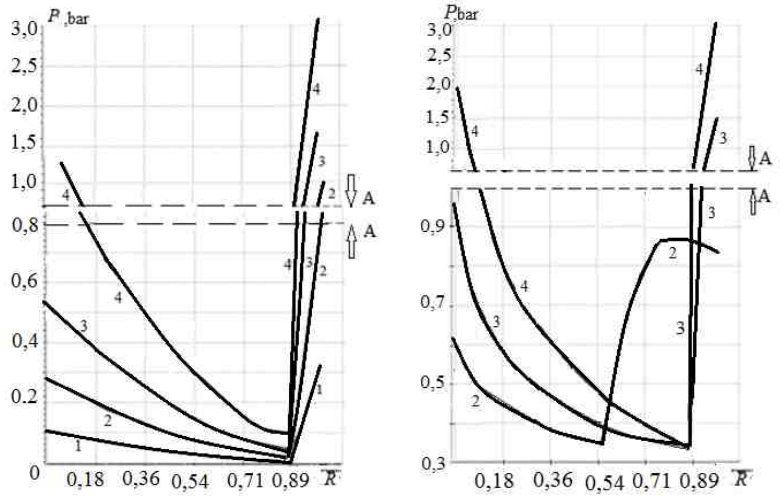

a) b)

Fig. 11 – Distribution of static pressure at the cutoff shortened nozzle with external pressure $P_н$ = 0.1 bar (a), $P_н$ = 1.0 bar (b) and inlet pressure P_0 = 20 (curve 1), 50 (curve 2), 100 (curve 3), 200 (curve 4) bar

Conclusions. 1. The wave structure of a supersonic gas flow in a shortened nozzle with an elliptical bell-shaped nozzle with a length equal to $l = \frac{l_{tip}}{L_S} = 0.86$ has been studied.

2. At low values of pressure at the nozzle inlet P_0<50 bar and external pressure $P_н$=1 bar, there is a developed separated zone with a large- and small-scale vortex in the area of the nozzle cutoff on the tip wall from the corner point of entry into the tip to its cut.

3. In the area of the first “barrel” of the gas flow, behind the cut of its inlet conical part, there is a “saddle-shaped” compression wave structure of low intensity. Its dimensions and intensity depend on the pressure P_0 at the inlet to the nozzle.

4. Behind the cut of the conical inlet (to the tip) section of the nozzle, there is a toroidal zone with an increased flow velocity, its longitudinal dimensions depend on the pressure P_0.

5. The pressure on the nozzle wall differs in the cases of separated and continuous (unseparated) flow on the nozzle wall. In the case of separated flow into the nozzle (at P_0 < 50 and $P_н$ = 1 bar), the pressure behind the corner entry point into the tip is a little lower (by ≈ 15 %) than the external pressure $P_н$. At P_0 > 100 bar and $P_н$ = 1 bar, the pressure on the tip wall changes almost in proportion to the pressure change at the nozzle inlet, retaining its character.

6. The static pressure in the cross section at the tip cutoff at $P_н$ = 0.1 bar is proportional to the pressure at the nozzle inlet. From the nozzle axis to $\approx 0.89\frac{R}{R_a}$, the pressure decreases monotonically to a value corresponding to the pressure at the nozzle inlet. Then it increases linearly to the value at the tip wall, also proportional to the nozzle inlet pressure.

7. At an external pressure of $P_н$ = 1 bar, the static pressure in the cross section at the tip cutoff at P_0 > 100 bar has the same character as at $P_н$ = 0.1 bar. At P_0 < 50 bar, the static pressure in the transverse section pressure decreases monotonically

up to the radius $\overline{R} \approx 0.57$. Higher up to the tip wall, the pressure monotonically increases to the value in the separated zone on the tip wall (~ 0.85 bar).

1. *Emelyanov V. N., Volkov K. N., Yakovchuk M. S.* Unsteady Flow in a Dual-Bell Nozzle with Displacement of an Extendible Section from the Initial to Working Position. Fluid Dynamics. 2022. Vol. 57. Suppl. 1. P. 35–45. https://doi.org/10.1134/S0015462822601267
2. *Génin Ch., Stark R.* Experimental Study on Flow Transition in Dual Bell Nozzles. Journal of Propulsion and Power. 2009. № 2. P. 497–502. https://doi.org/10.2514/1.47282
3. *Volkov K. N., Emel'yanov V. N.,. Chernyshov P. S*. Flow dynamics and acoustics of the gas jet emanating from a conical nozzle into an immersed space. Journal of Engineering Physics and Thermophysics. 2022. Vol. 95, No. 2. P. 409–420. https://doi.org/10.1007/s10891-022-02495-x
4. *Martelli E., Nasuti F., Onofri M*. Numerical parametric analysis of dual-bell nozzle flows. AIAA. 2007. Vol. 45, № 3. P. 640–650. https://doi.org/10.2514/1.26690
5. *Ihnatiev O. D., Pryadko N. S., Strelnikov G. O., Ternova K. V.* Gas flow in a shortened laval nozzle with a bell-shaped nozzle. Technical mechanics. 2022. № 2. P. 39–46. https://doi.org/10.15407/itm2022.02.039
6. *Genin C., Stark R., Haidn O., Quering K., Frey M.* Experimental and numerical study of dual bell nozzle flow. Progr. Flight Phys. 2013. Vol. 5. P. 363–376. https://doi.org/10.1051/eucass/201305363
7. *Nasuti F., Onofri M., Martelli E.* Role of wall shape on the transition in axisymmetric dual-bell nozzles. J. Propul. Power. 2005. Vol. 21. №. 2. P. 243–250. https://doi.org/10.2514/1.6524
8. *Vermaa S. B., Haidnb O.* Unsteady shock motions in an over-expanded parabolic rocket nozzle. Aerospace Science and Technology. 2014. Vol. 39. P. 48–71. https://doi.org/10.1016/j.ast.2014.08.003
9. *Asha G., Naga Mohana D., Sai Priyanka K., Govardhan D.* Design of Minimum Length Nozzle Using Method of Characteristics. International Journal of Engineering Research & Technology (IJERT). 2021. Vol. 10. Issue 05. P. 490–495.
10. *Joshi P., Gandhi T., Parveen S.* Critical Designing and Flow Analysis of Various Nozzles using CFD Analysis. International Journal of Engineering Research & Technology (IJERT). 2020. Vol. 9. Issue 02. P. 421–424. https://doi.org/10.17577/IJERTV9IS020208
11. *Strelnikov G., Pryadko N., Ihnatiev O., Ternova K.* Choice of a turbulence model for modeling complex flows in rocket engine nozzles. Novel Research in Sciences. 2022. Vol. 10. Issue 5. P. 1–5.
12. *Abramovich G. N.* Applied gas dynamics. Edition 5. M.: «Nauka». 1991. 600 p.

Received on February 6, 2023,
in final form on March 30, 2023